Kinetics of assembly and dissociation of the mitochondrial creatine kinase octamer. A fluorescence study

ARTICLE *in* BIOCHEMISTRY · JANUARY 1994

Impact Factor: 3.02 · DOI: 10.1021/bi00213a024 · Source: PubMed

2 AUTHORS:

Markus Gross
ETH Zurich
336 PUBLICATIONS **10,890** CITATIONS
SEE PROFILE

Theo Wallimann
ETH Zurich
287 PUBLICATIONS **15,202** CITATIONS
SEE PROFILE

Kinetics of Assembly and Dissociation of the Mitochondrial Creatine Kinase Octamer. A Fluorescence Study†

Martin Gross* and Theo Wallimann

Swiss Federal Institute of Technology, Institute for Cell Biology, ETH-Hönggerberg, CH-8093 Zürich, Switzerland

Received August 27, 1993; Revised Manuscript Received October 19, 1993•

ABSTRACT: The dissociation of octameric mitochondrial creatine kinase (Mi-CK) into dimers induced by the transition-state analogue complex (TSAC) mixture (creatine + Mg^{2+} + ADP + NO_3^-) is accompanied by a large (25.2%) decrease in Trp fluorescence. This effect is caused by a Trp residue situated at the dimer–dimer interface within the octamer, which becomes susceptible to solvent quenching upon octamer dissociation. Octamer formation, induced by adding excess EDTA to TSAC-dissociated Mi-CK, involves a transient tetrameric species, whereas the dissociation reaction proceeds in a one-step, all-or-none fashion. From fluorescence spectroscopic investigations of the octamer formation and dissociation reactions, a first-order dissociation rate constant of 0.19 min^{-1} and a bimolecular association rate constant of 318 M^{-1} s^{-1} at 30 °C were obtained. The octamers formed after EDTA addition can be dissociated again by lowering the temperature to 4 °C, indicating a substantial hydrophobic contribution to the interactions stabilizing the octamer.

Creatine kinase (CK,[1] EC 2.7.3.2) catalyzes the reversible phosphoryl transfer from phosphocreatine to ADP, thus exerting an important metabolic function in tissues of high and fluctuating energy requirement. The enzyme is found in tissue-specific (M, muscle type, and B, brain type) as well as in compartment-specific (cytosolic and mitochondrial) isoforms (Jacobs et al., 1964; Eppenberger et al., 1983; Wallimann et al., 1992). The cytosolic ones are homo- or heterodimeric (MM-, BB-, or MB-CK), whereas the mitochondrial creatine kinases (Mi-CK) form octamers (Quemeneur et al., 1988; Schlegel et al., 1988b; Schnyder et al., 1988). Mi-CKs are exclusively found in the mitochondrial intermembrane compartment, being peripherally attached to the inner membrane. This localization enables the enzyme to utilize preferentially the intramitochondrially produced ATP for the synthesis of phosphocreatine (Jacobus & Lehninger, 1973; Saks et al., 1985), which, in turn, can be exported into the cytosol where it is used for the regeneration of ATP by the cytosolic isoforms at the sites of energy demand. This interplay between the cytosolic and mitochondrial CKs, with the easily diffusible (phospho)creatine serving as an energy shuttle system between the cellular compartments in addition to providing its energy-buffering function, is referred to as the "phosphocreatine circuit" [reviewed in Wallimann et al. (1992) and Wyss et al. (1992)].

The Mi-CK octamer consists of four stable homodimers [M_r(dimer) = 84 000], which themselves cannot be further dissociated into monomers under physiological conditions. In electron micrographs, the octamer displays *P*422 symmetry, giving the appearance of a cube-shaped assembly with the four elongated dimers grouped around the fourfold axis (Figure 1) (Schnyder et al., 1988). The "top" and "bottom" faces appear to be identical and have been found to attach to all commonly used electron microscopy supports as well as to each other in linear aggregates of multiple octamers (Schnyder et al., 1991). Therefore, they are also believed to be the faces that interact with lipid membranes; moreover, it has been shown that Mi-CK octamers, compared to the dimers, bind to lipid membranes with higher affinity (Rojo et al., 1991b) and are capable of mediating the formation of contact sites between the mitochondrial membranes *in vitro* (Rojo et al., 1991a). These findings suggest that the octameric structure represents an adaptation of the mitochondrial CK isotypes to their specific localization and function. Since Mi-CK is enriched at the mitochondrial contact sites (Biermans et al., 1990; Kottke et al., 1991; Wegmann et al., 1991), it is tempting

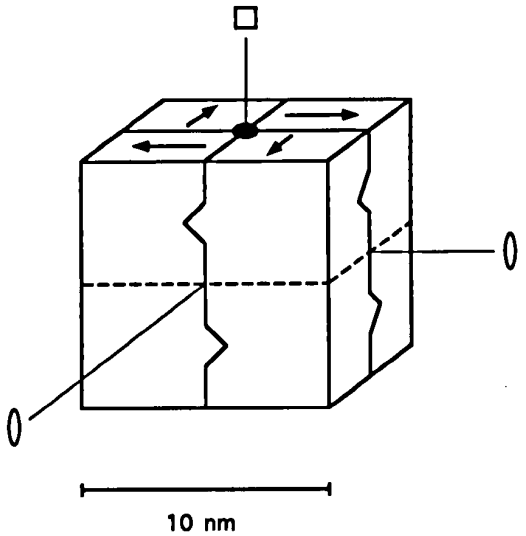

FIGURE 1: Schematic representation of the symmetry features of the Mi-CK octamer. Arrows on top indicate the cyclic arrangement of dimers around the 4-fold symmetry axis. Dashed lines indicate monomer boundaries. The central channel running along the 4-fold axis is indicated on the top surface only. Notches symbolize the asymmetric dimer–dimer contacts.

† This work was supported by grants from the Helmut-Horten-Stiftung and the Swiss National Science Foundation (SNF Grant 31-33907.92 to T.W.).

* To whom correspondence should be addressed. Telephone: 41-1-633-3391. Fax: 41-1-371-2894.

• Abstract published in *Advance ACS Abstracts*, December 1, 1993.

[1] Abbreviations: 2-ME, 2-mercaptoethanol; BSA, bovine serum albumin; CK, creatine kinase; EDTA, ethylenediaminetetraacetic acid; Mi_b-CK, chicken sarcomeric mitochondrial creatine kinase; TSAC, transition-state analogue complex; Y-GAPDH, yeast glyceraldehyde-3-phosphate dehydrogenase.

0006-2960/93/0432-13933$04.00/0

to speculate that it could serve as the connecting module between the adenine nucleotide translocator in the inner membrane and porin in the outer membrane. Such a vectorial protein complex could form an efficient "energy channel" that combines the translocation of energy equivalents with their interconversion from the nucleotide to the creatine carrier system (Wyss & Wallimann, 1992).

The equilibrium between Mi-CK dimers and octamers is influenced by a variety of parameters; Mi-CK is isolated from mitoplasts mainly in the octameric form, which also predominates (≥80%) in solutions of high (≥1 mg/mL) protein concentration. When octameric Mi-CK is diluted, the oligomeric equilibrium slowly shifts (for the chicken sarcomeric Mi_b-CK, at 4 °C, $t_{1/2}$ = 1–2 months) toward higher dimer proportions. When the protein concentration is raised again, a fast reassembly of octamers is observed. High pH, low temperature, and the presence of organic solvents (e.g., ethylene glycol) shift the dimer–octamer equilibrium toward the dimeric side (Schlegel, 1989; Wyss et al., 1992).

A *fast* dissociation of the octamer ($t_{1/2}$ = several minutes), however, can be induced by addition of a transition-state analogue complex (TSAC) mixture, consisting of ADP, magnesium chloride, creatine, and potassium nitrate, to a diluted Mi-CK sample (Marcillat et al., 1987; Schlegel et al., 1988a). This strong effect of the CK substrates, together with the observation of a wide tissue- and species-dependent variability in octamer stability (Wyss et al., 1992), points to a possible role of the dimer–octamer equilibrium in metabolic regulation and adaptation (Wallimann et al., 1992). Therefore, a detailed fluorescence spectroscopic analysis of the kinetics of octamer formation and dissociation is presented in this paper.

In several previous reports, the specific fluorescence quenching of an active site tryptophan (Trp) residue by the nucleotide substrate has been described for MM-CK (Vasak et al., 1979; Messmer & Kägi, 1985). In the Mi-CK octamer, a lower active site accessibility in comparison to that of the dimer has been suggested from thiol modification and enzyme kinetic studies (Belousova et al., 1986; Fedosov & Belousova, 1989). We therefore expected a decrease in intrinsic protein fluorescence to accompany the dissociation of Mi-CK octamers in the presence of adenine nucleotide, thereby allowing a direct monitoring of transitions between the octameric and dimeric states of Mi-CK. A large fluorescence decrease during the TSAC-induced octamer dissociation was indeed observed, though for different reasons than anticipated. This fluorescence effect could be exploited to investigate extensively the kinetics of quaternary structure transitions as well as the characteristics of the dimer–dimer interactions, resulting in a mechanistic model describing the octamer formation and dissociation processes.

MATERIALS AND METHODS

Overexpression and Purification of Mi_b-CK. Chicken sarcomeric mitochondrial creatine kinase (Mi_b-CK) was overexpressed in the *Escherichia coli* strain BL21(DE3)pLysS transformed with the expression vector pRF23, and the protein was purified as described (Furter et al., 1992). In short, lysates were obtained by sonication of the cells, and the enzyme was isolated by a two-step protocol, including Blue Sepharose affinity chromatography and cation-exchange chromatography on a Mono S HR5/5 FPLC column (Pharmacia). Concentrated Mi_b-CK stocks were stored in Mono S elution buffer at −80 °C and were stable after thawing for several weeks at 4 °C. CK activity was routinely assayed by the pH-stat method (Wallimann et al., 1984), measuring the rate of the reverse reaction (ATP production). Protein concentrations were determined with the Bio-Rad dye adsorption assay (Bradford, 1976), using BSA as standard.

Quantitation of Oligomeric Species. The distribution of oligomeric species in Mi_b-CK samples was determined by gel permeation chromatography on a Superose 12 FPLC column (Pharmacia) at 4 °C, using Superose running buffer (50 mM sodium phosphate, 150 mM NaCl, 2 mM 2-ME, and 0.2 mM EDTA, pH 7.0). The separations were performed at a flow rate of 0.7 mL/min; the last Mi-CK fraction (dimeric) thus was eluted after 20 min. Peak areas in the elution profiles were quantitated by graphical integration.

Fluorescence Spectroscopy. Steady-state fluorescence measurements were performed on a SPEX Fluorolog-2 instrument, equipped with a 450-W xenon arc lamp as excitation source. All data were acquired in the ratio mode, using a rhodamine-B reference quantum counter, and spectra were corrected for variations in the responses of the emission gratings and the detector. Magnetically stirred 1-cm quartz cells (minimum sample volume, 2.1 mL) were positioned in a thermostated sample holder, and fluorescence emission was measured with rectangular excitation. For emission spectra, slit widths of 3.4 nm (excitation) and 1.7 nm (emission) were chosen; Trp fluorescence was excited at 287 nm (i) to minimize tyrosine excitation and (ii) to keep the water Raman peak (observed at 31 nm distance from the excitation wavelength) out of the protein fluorescence maximum. Spectra were routinely measured at 30 °C with a protein concentration of 50 μg/mL in Mono S buffer (25 mM sodium phosphate, 50 mM NaCl, 2 mM 2-ME, and 0.2 mM EDTA, pH 7.0).

Fluorescence Quenching Experiments. Fluorescence quenching titrations with potassium iodide, potassium nitrate, and acrylamide were performed at 30 °C and 50 μg/mL protein concentration in Superose running buffer. Excitation and emission wavelengths were set at 295 and 340 nm, respectively. In the case of acrylamide and KNO_3, the data were corrected for inner filter effects by measuring the compounds' absorbance at the excitation and emission wavelengths and calculating the correction factors according to Parker and Barnes (1957). Correction for ionic strength effects was achieved in the case of KI and KNO_3 by relating the measured emission intensities to the values obtained by parallel titrations with KCl. The quenching data were plotted according to the Stern–Volmer equation,

$$F_0/F = 1 + K_{SV}[Q]$$

with F_0 being the fluorescence emission intensity in the absence of quencher, F being the emission intensity in the presence of the quencher at a concentration [Q], and K_{SV} representing the Stern–Volmer constant, which is a measure for the susceptibility of a given fluorophore to dynamic quenching by a certain compound.

Octamer Dissociation Assay. Mi_b-CK stock solution, containing ≥95% octamers, was diluted to a final assay concentation of 50 μg/mL and equilibrated for 10 min at 30 °C in the fluorescence cuvette (a small fluorescence decrease, due to protein adsorption to the quartz walls, occurred during the first 5 min). Fourfold concentrated, prewarmed TSAC mixture (final concentrations: 4 mM ADP, 5 mM $MgCl_2$, 20 mM creatine, and 50 mM KNO_3) was added to the stirred protein solution to initiate octamer dissociation. Trp fluorescence readings in short intervals (5–15 s) were immediately started, with the excitation and emission wavelengths set at 295 and 340 nm, respectively. The excitation

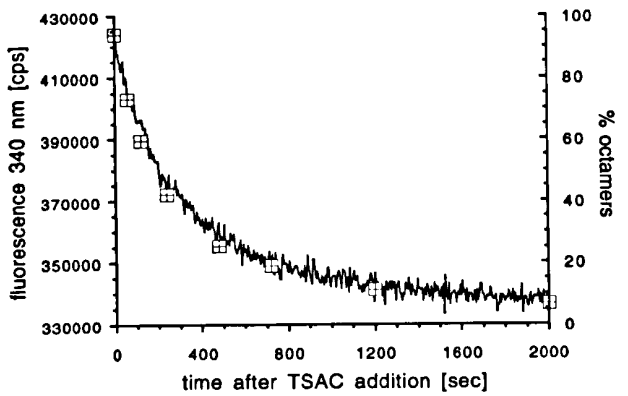

FIGURE 2: Dissociation of the Mi-CK octamer: Comparison of Trp fluorescence trace (—) and corresponding octamer percentages, measured by gel permeation chromatography (⊞) after TSAC addition at 30 °C. Excitation wavelength, 295 nm.

slit width was reduced to 0.7 nm to avoid significant photobleaching of the samples during measurements lasting up to 2 h. Octamer dissociation was additionally assayed by incubating separate samples of Mi_b-CK with TSAC mixture under identical conditions for defined periods, stopping the dissociation by diluting below a critical TSAC concentration (found to be approximately half of the original concentration, the amount of ADP being limiting), and immediately applying the samples to the Superose column.

Octamer Formation Assay. Mi_b-CK was dissociated at various protein concentrations by overnight incubations at room temperature with the TSAC substrates in Superose running buffer. Residual octamer contents were determined in aliquots by gel permeation chromatography. After equilibration of the dissociated samples at 30 °C in the fluorescence cell, reoctamerization was started by the addition of excess EDTA (final concentration, 25 mM), and Trp fluorescence was monitored as described for the dissociation assay. Aliquots were taken after defined periods to determine the corresponding octamer contents by gel permeation chromatography (see above). After 4 h of incubation at 30 °C, aliquots of the samples were stored at room temperature and at 4 °C for a further 5 days to determine the equilibrium octamer percentages at these temperatures.

RESULTS

Octamer Dissociation. The TSAC-induced dissociation of the Mi-CK octamer is accompanied by a decrease in Trp fluorescence, as can be seen from the comparison of the fluorescence trace with the corresponding octamer contents determined by gel permeation chromatography (Figure 2). In the experiment shown, the octamer population decreased from 96% to 6% within less than 30 min; extrapolating the fluorescence effect to a 100% octamer to dimer conversion gives a difference in intrinsic protein fluorescence of 25.2% between octameric and dimeric Mi_b-CK. The time course of the fluorescence decrease could be perfectly fitted to a single-exponential rate law, with a decay constant k of 0.19 min^{-1}, corresponding to a half-life time of 3.7 min, at 30 °C. Identical decay rates were found over a protein concentration range from 0.01 to 0.2 mg/mL (not shown), indicating a first-order process. In the gel permeation profiles, only two species, octameric and dimeric Mi-CK, could be detected during the dissociation reaction, eluting at 10.7 and 13.3 mL, respectively. Interestingly, already at 2-fold dilution of the TSAC mixture, the dissociation rate is drastically reduced (almost no detectable fluorescence change on a time scale of minutes; not shown); a 2-fold dilution is used to stop the dissociation reaction prior to sample application on the Superose column (see Materials and Methods). This steep dependence of the dissociation reaction on the TSAC substrate concentration could be due to a cooperative effect: possibly, a critical number of active sites per octamer has to be occupied by the TSAC substrates in order to induce the dissociation into dimers; if the number of protomers in the transition-state conformation is below the threshold, the octamer is not sufficiently destabilized.

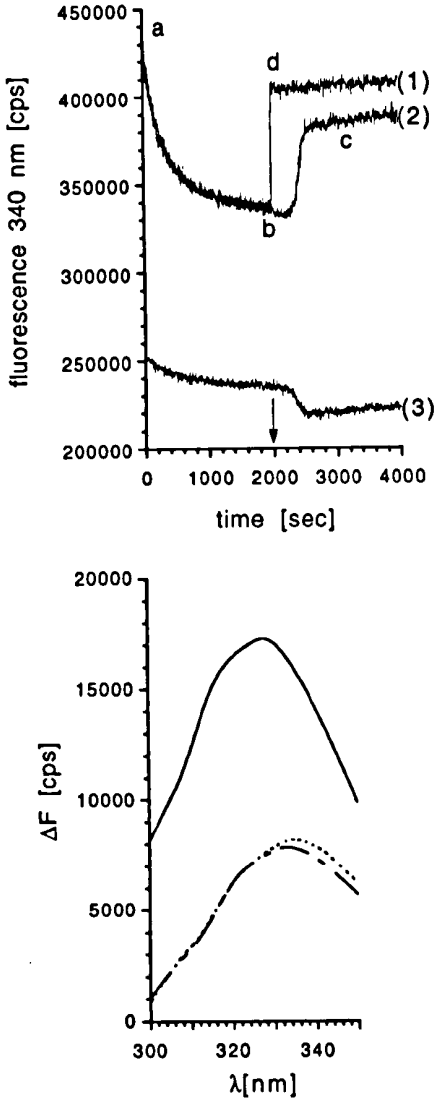

FIGURE 3: Comparison of Trp fluorescence changes caused by octamer dissociation and by active site Trp quenching. (A) Octamer dissociation by TSAC and subsequent addition (arrow) of 25 mM EDTA (curve 1) or 3 units of apyrase (curve 2). Curve 3: Same experiment as curve 2 but in the presence of 1 M acrylamide. (B) Difference fluorescence emission spectra: —, spectrum recorded directly after addition of TSAC substrates minus spectrum of the same sample recorded after 30-min TSAC incubation (a – b in panel A); – – –, difference spectrum of TSAC-dissociated Mi-CK after and before apyrase incubation (c – b); - - -, difference spectrum of TSAC-dissociated Mi-CK after and before addition of 25 mM EDTA (d – b).

Origin of the Fluorescence Decrease Associated with Octamer Decay. Apyrase (obtained from Sigma) is an enzyme which hydrolyzes ADP to AMP and P_i. When this enzyme was added to the TSAC-dissociated samples, a fast increase in protein fluorescence was detected, indicating a dequenching of the active site Trp residue (Figure 3A). The time period

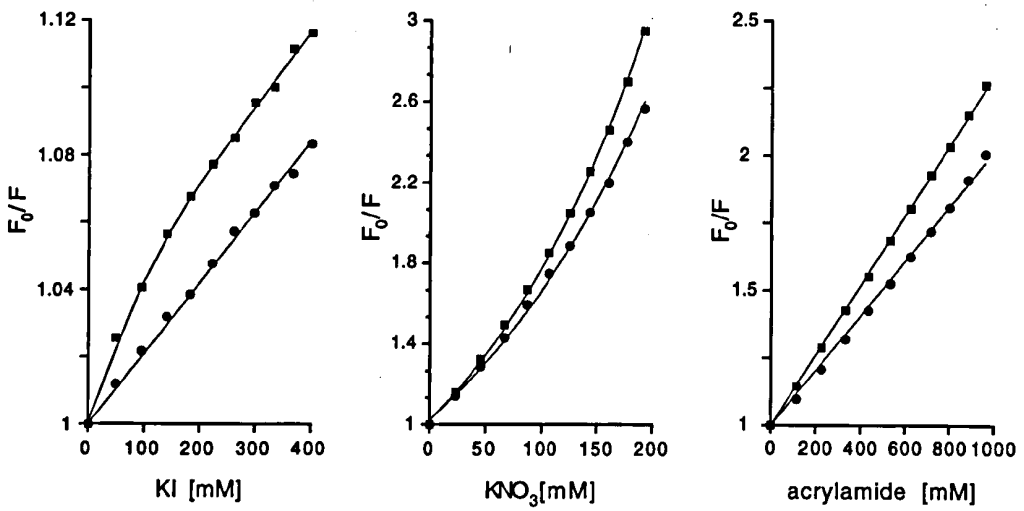

FIGURE 4: Differences in Trp quenchability of Mi-CK dimers and octamers. Fluorescence quenching titrations of 96% octameric (●) and 74% dimeric Mi-CK (■) with KI, KNO_3, and acrylamide (Stern–Volmer plots). Dimeric Mi-CK was obtained by TSAC dissociation and subsequent extensive dialysis to remove TSAC substrates. Curves are corrected for ionic strength and inner filter effects (see Materials and Methods).

required to achieve this increase in fluorescence was dependent on the amount of apyrase added (not shown). A similar, but instantaneous, effect could be achieved by the addition of excess (25 mM) EDTA, which by withdrawing the Mg^{2+} ions also destroys the TSAC. (At the low Mi-CK concentration employed, no reoctamerization took place during the time of observation.) When the octamer dissociation assay is performed in the presence of acrylamide, which is a particularly potent fluorescence quencher, subsequent apyrase addition causes a further fluorescence *decrease*, indicating that the removal of ADP from the active site results in a deshielding of the Trp residue, leading to even stronger quenching by acrylamide (Figure 3A).

Several observations suggest that the fluorescence decrease occurring during octamer dissociation is independent of the specific quenching of the active site Trp residue by the TSAC substrates. First, the fluorescence increases caused by either apyrase or EDTA addition were of a significantly smaller magnitude than the effect resulting from octamer dissociation; furthermore, similar fluorescence enhancements by EDTA or apyrase addition could also be produced with the octameric protein (not shown). In fact, fluorescence emission difference spectra (Figure 3B) reveal that the Trp residue involved in the active site quenching effect exhibits spectral characteristics distinct from those of the Trp residue involved in the oligomeric state dependent fluorescence effect. The difference spectrum resulting from octamer dissociation, obtained by comparing the emission spectra upon addition of the TSAC substrates and 30 min thereafter, has its maximum at 327.5 nm. This is clearly distinguishable from the difference spectra arising from active site Trp quenching, obtained by the comparison of the spectra before and after apyrase or EDTA addition; the maxima of these difference spectra are at 333 (apyrase) and 334.5 nm (EDTA). This suggests that the fluorescence decrease observed during octamer dissociation is *not* due to enhanced static quenching of the active site Trp by ADP, but that it originates from a different Trp residue situated in a more hydrophobic environment.

To further demonstrate that the fluorescence decrease accompanying the TSAC-induced dissociation is due to quenching of a Trp residue which is different from the one located at the active site, the quenching of predominantly octameric samples by KI, KNO_3, and acrylamide was compared to that of predominantly dimeric samples. The quenching titrations (Figure 4) clearly demonstrate the generally enhanced quenchability of the dimeric Mi-CK intrinsic fluorescence compared to that of the octameric form (all Stern–Volmer plots are steeper for the dimers), irrespective of the type of quencher used, indicating that a Trp residue exposed only in the dimers is susceptible to *nonspecific* quenching. KI quenching of dimeric Mi-CK results in a characteristically downward curved Stern–Volmer plot, which has also been observed with MM-CK; the reason for this is assumed to be the differential accessibility of Trp residues for the polar quencher (Messmer & Kägi, 1985). In contrast, the octamer exhibits a linear Stern–Volmer plot upon KI quenching. Since a large variety of conditions can lead to apparently linear curves (Eftink & Ghiron, 1981), the interpretation of this finding is not straightforward. In the case of KNO_3, the plots for both dimeric and octameric Mi-CK curve strongly upward, which may be an indication for a large static component in the quenching mode of the nitrate ion. NO_3^- is believed to occupy the γ-phosphate binding site in the transition-state analogue complex (Milner-White & Watts, 1971); consequently, a static quenching of the active site Trp residue by the planar anion is likely. The extremely high quenching efficiency of nitrate in comparison to iodide may be another indication for a more specific binding of this anion to CK. At 50 mM KNO_3, which is the concentration present in the TSAC mixture, the difference in quenchability between octamers and dimers is not quite as large as expected from the dissociation assay. This can be explained by the fact that the "dimeric" Mi-CK samples used for quenching titrations were not completely dimeric (74% measured) and that an unknown amount of tetramers was probably present (see below).

Since the Trp residue that becomes accessible upon octamer dissociation can be quenched nonspecifically, dissociation of the octamer by ≥0.5 M KI leads to a fluorescence decrease very similar to that observed using the TSAC mixture (not shown). For the same reason, Stern–Volmer plots of KI quenching experiments with octameric Mi-CK sharply curve upward above KI concentrations of about 0.5 M, since the octamers slowly begin to dissociate (not shown).

The fluorescence decrease observed upon octamer dissociation in the presence of the TSAC mixture is mainly due to the nitrate ion. When Mi-CK octamers are dissociated in the absence of nitrate (a slow dissociation with a half-life time

of about 2 h can be achieved with the TSAC mixture lacking KNO_3 at 30 °C), Trp fluorescence only decreases by approximately 7% (not shown).

Octamerization Kinetics. The destruction of the transition-state analogue complex can be achieved either by apyrase hydrolysis of the ADP or by complexing the Mg^{2+} with excess EDTA. Both methods, when applied to TSAC-dissociated Mi-CK samples at protein concentrations ≥0.1 mg/mL, lead to reoctamerization of the enzyme. The concomitant Trp fluorescence increase can be used to study the kinetics of octamer assembly. When apyrase is employed to hydrolyze the ADP, the onset of reoctamerization cannot clearly be defined, since the starting point lies within the initial fluorescence increase caused by the relatively slow enzymatic dequenching of the active site Trp; therefore, the instantaneous TSAC destruction by EDTA was chosen for the fluorescence spectroscopic monitoring of the kinetics of octamer formation. Due to proton release from EDTA, complexing of the Mg^{2+} ions shifted the pH of the assay solution from 7.0 to 6.9.

The time course of the observed fluorescence increases is strongly dependent on protein concentration (Figure 5A); below a threshold concentration of 0.1 mg/mL, no fluorescence increase at all is observable within the detection limits; at 0.1 mg/mL, a lag phase precedes the sudden onset of the rise in fluorescence.

To determine the relation between the fluorescence changes and the increase in octamer content, samples were removed from the cuvette at defined time points, and the octamer percentages were directly determined by gel permeation chromatography (shown for the 0.2 mg/mL sample in Figure 5B). In the gel permeation profiles, small amounts (about 3–6%) of a third oligomeric species, eluting at 12.2 mL, were detected (Figure 5B); this intermediate probably represents a tetramer (calibration of the Superose column with globular reference proteins resulted in a calculated M_r of 132 000, or a Stokes radius of 48 Å). After 3 h of reoctamerization, when the reaction approached equilibrium, the proportion of tetramers detected was greatest in samples with the lowest protein concentrations; for all samples, the amount of tetramers detected tended to decrease slightly during the octamerization reaction, suggesting a transient accumulation of the tetrameric species during the initial reaction phase.

In contrast to the dissociation experiments, where a direct correspondence was seen between the fluorescence decrease and the decreasing octamer content (see Figure 2), significant deviations from a proportional correlation were found when the measured increase in octamer percentage was compared to the fluorescence increase upon reoctamerization. At 0.1 mg/mL protein concentration, the observed fluorescence increase was about 4-fold higher than one would have expected from the corresponding increase in octamers. However, at 0.4 mg/mL, the fluorescence increase appeared to correlate directly with the increase in octamer percentage. This concentration-dependent discrepancy between the observed fluorescence signal and the actual octamer content strongly suggests that, in the octamerization reaction, the tetramer is formed as an unstable intermediate, causing a fluorescence change. Due to its instability, however, the majority of this species escapes detection by gel permeation chromatography, since it mainly appears in the dimer fraction. However, at high protein concentrations, most of the tetramers immediately proceed in the reaction sequence to form stable octamers, so that the tetramer population always stays negligibly low.

When the reoctamerized protein samples were cooled to 4 °C after the assay (Figure 5C), the octamers slowly (with a

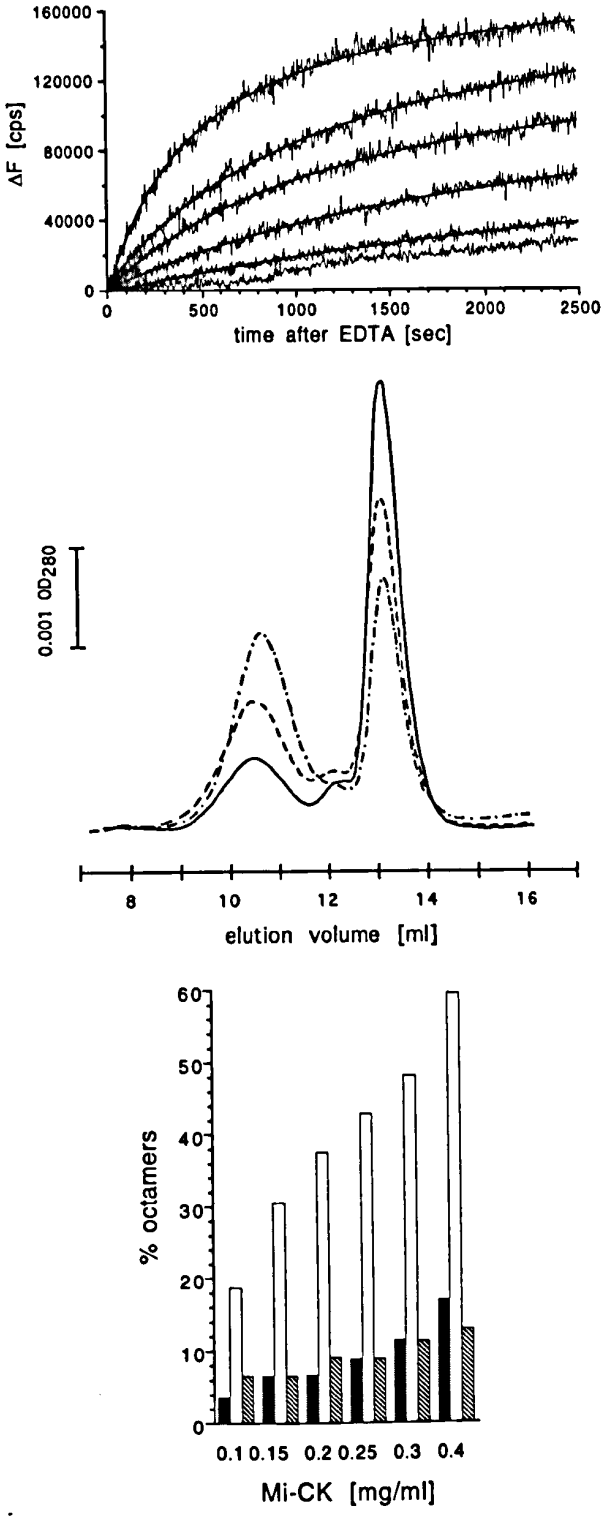

FIGURE 5: Mi-CK octamer formation. (A) Fluorescence traces observed during EDTA-induced reoctamerization of TSAC-dissociated Mi-CK at 30 °C. Total protein concentrations from bottom to top curve: 0.1, 0.15, 0.2, 0.25, 0.3, and 0.4 mg/mL; —, least-squares fits according to eq 8, with fixed $[A]_0$ and F_0. (B) Exemplary gel permeation profiles of reoctamerization samples from assay at 0.2 mg/mL protein concentration taken after 0 (—), 900 (- - -), and 10800 s (- · -). (C) Equilibrium octamer percentages in Mi-CK samples after overnight TSAC incubation at room temperature (before octamerization assay) (solid bars) and after octamerization assay (25 mM EDTA, 4 h, 30 °C) and additional storage for 5 days (to reach equilibrium) at room temperature (open bars) or, alternatively, at 4 °C (hatched bars). Octamer contents were determined by gel permeation chromatography.

half-life time of approx. 1 h) dissociated again to the initial state, showing that the dimer–octamer transition in the presence of TSAC mixture + EDTA can be completely reversed by lowering the temperature.

To analyze the octamer formation kinetics in more detail, an irreversible bi–bi association mechanism of the type

$$2A \xrightarrow{k_1} B; \quad 2B \xrightarrow{k_2} C$$

was assumed, with A, B, and C representing the dimeric, tetrameric, and octameric Mi-CK species, respectively. The corresponding rate equations are

$$d[A]/dt = -k_1[A]^2 \tag{1}$$

$$d[B]/dt = \frac{k_1}{2}[A]^2 - k_2[B]^2 \tag{2}$$

$$d[C]/dt = \frac{k_2}{2}[B]^2 \tag{3}$$

This set of differential equations has been solved analytically (Chien, 1948), the expressions for the time-dependent concentrations of A, B, and C being

$$[A] = [A]_0/\tau \tag{4}$$

$$[B] = \frac{[A]_0}{2}\frac{1}{\kappa\tau}\left[\mu + 1 - \frac{2\mu}{1 + \frac{\mu - 1}{\mu + 1}\tau^{\mu}}\right] \tag{5}$$

$$[C] = \frac{1}{2}\left[\frac{[A]_0}{2} - \frac{[A]}{2} - [B]\right] \tag{6}$$

where

$$\tau = 1 + [A]_0 k_1 t; \quad \kappa = k_2/k_1; \quad \mu = (1 + 2\kappa)^{1/2}$$

From the data presented above and from the symmetry features of the Mi-CK octamer (see Figure 1) it can be concluded that, upon the formation of a dimer–dimer contact, two Trp residues (one per dimer) become buried in the interface. Consequently, four Trp residues (again, one per dimer) must become protected from solvent quenching when an octamer is formed out of two tetramers. Thus, the fluorescence increase per octamer formed should be exactly twice the effect produced by the formation of a tetramer.

Therefore, by introducing a proportionality constant, f, which represents the fluorescence increase per mole of dimer–dimer contacts formed, an expression for the time-dependent fluorescence intensity can be obtained:

$$F = F_0 + ([B] + 2[C])f \tag{7}$$

where F_0 is the fluorescence intensity at $t = 0$.

When eqs 4–6 are substituted into eq 7, the concentration of the intermediate B cancels out, simplifying the expression to

$$F = F_0 + \left(\frac{[A]_0}{2} - \frac{[A]_0}{2(1 + [A]_0 k_1 t)}\right)f \tag{8}$$

Now, the fluorescence trace can be regarded to represent the sum of the effects caused by tetramer *and* octamer formation, irrespective of the distribution between the two species. Alternatively, eq 8 can be interpreted as a description of the *disappearance of dimers*, which has to be a bimolecular process in any case. This further implies that the fluorescence traces do not contain any information about the consecutive reaction(s) following the formation of tetramers; in particular, k_2 cannot be deduced, and it cannot be decided whether an additional reaction step (the formation of hexamers) is involved. On the other hand, fitting of the experimental data to this equation only requires the variation of two parameters, which are k_1 and f, since F_0 can be taken directly from the fluorescence curves, and the initial dimer concentrations can be independently determined by gel permeation chromatography.

When the measured fluorescence traces are fitted to eq 8, good agreement of the data with the calculated curves is achieved (Figure 5A), with no apparent systematic deviations. The only case where the fitting procedure cannot be applied is at the lowest protein concentration (0.1 mg/mL), where an initial lag phase occurs. This probably is a result of the simplifying assumption of an *irreversible* reaction; since the tetramer has to be regarded as an unstable species, a reverse reaction rate constant, k_{-1}, comes into play, which is no longer negligible in the lower protein concentration range. The consequence of this is a more complex behavior of the system which cannot be accomodated by eq 8.

The rate constant k_1 was found to be 318 ± 130 M^{-1} s^{-1} at 30 °C (the molar concentration being expressed in units of the 84-kDa dimer), and f is determined as 37.4 ± 2.5% relative fluorescence increase accompanying the association of two dimers. This is in good agreement with the value for f of 33.7% which can be predicted from the fluorescence decrease observed during octamer dissociation (a 25.2% *decrease* corresponds to a relative *increase* of 33.7%). Standard deviations for k_1 in the individual fits were 4% or less; the relatively high error of ±130 M^{-1} s^{-1} results from averaging the k_1 values over the concentration range from 0.15 to 0.4 mg/mL. Note, for comparison with other data in the literature, that in some cases a different definition of k_1, with $d[A]/dt = -2k_1[A]^2$, is used. Such k_1 values have to be divided by 2 to compare them with the data presented here.

DISCUSSION

The tryptophan fluorescence of CK has previously been exploited for probing the binding of purine nucleotides to the enzyme's active site. Here, we present another application of intrinsic protein fluorescence spectroscopy, which is employed to study the oligomeric transitions specific for the mitochondrial CK isoenzymes.

When the Mi-CK octamer is dissociated into dimers by adding the TSAC substrate mixture, a concomitant Trp fluorescence decrease is observed. The 25.2% difference between octameric and dimeric Mi-CK intrinsic fluorescence originates from the nonspecific quenching by NO_3^- ions of a Trp residue which becomes exposed to the solvent during the octamer decay. (When no quenching agents are present, the fluorescence of dimeric Mi-CK is slightly *higher* than in the octameric state; data not shown.) The environment of the affected Trp residue in the octamer appears to be very hydrophobic, as can be concluded from the difference spectrum exhibiting its maximum at 327.5 nm (Burstein et al., 1973; Eftink & Ghiron, 1976). Since it is generally known that at the interfaces of protein–protein contacts hydrophobic, especially aromatic, amino acid residues are accumulated to form hydrophobic interaction patches (Jaenicke & Rudolph, 1986; Janin & Chothia, 1990), it is tempting to assign the Trp residue producing the observed effect to such a hydrophobic contact area. The cytosolic CKs possess four conserved Trp residues per monomer. Only one of these Trp residues, located

at the active site, has been reported to be exposed at the dimer surface (the presence of excess adenine substrate completely abolishes Trp quenchability by KI) (Messmer & Kägi, 1985). We have shown that this active site Trp in Mi-CK has distinct spectral properties compared to the Trp quenched upon octamer dissociation; therefore, none of the four conserved Trp residues is likely to be involved in dimer–dimer contact formation in the Mi-CK octamer. However, all known primary sequences of Mi-CK isoenzymes exhibit an additional Trp at position 264 which is replaced by histidine in all M-CKs and tyrosine in all B-CKs; thus, the fifth Trp residue in Mi-CK may represent an isotype-specific adaptation which is correlated with the ability to form octamers and is likely to be the residue which is nonspecifically quenched upon octamer decay.

A further indication for a large hydrophobic contribution to the octamer-stabilizing forces comes from the finding that the EDTA-induced octamerization can be reversed by lowering the temperature (Figure 5C). A strikingly similar behavior has been found for the tetrameric yeast glyceraldehyde-3-phosphate dehydrogenase (Y-GAPDH) (Stance & Deal, 1969; Bartholmes & Jaenicke, 1975, 1978), which also undergoes reversible cold dissociation in the presence of nucleotide (ATP). (However, in this case ATP is not a substrate but a competitive inhibitor of the enzyme.) On the other hand, by replacing or deleting charged amino acids from the N-terminus of Mi_b-CK, a large general destabilization of the octameric structure can be achieved (P. Kaldis, personal communication). Provided that these residues are directly involved in the formation of intersubunit contacts, it can be concluded that the stability of the octameric state of Mi-CK is the result of a subtle interplay between polar and nonpolar interactions which are reflected by the observed ligand and temperature effects; the TSAC substrates in the absence of Mg^{2+} (in the presence of excess EDTA) appear to weaken selectively the polar interactions, thereby leading to the observed cold dissociation of the octamer.

The TSAC-induced decay of the Mi-CK octamer probably is a one-step dissociation process; this can be inferred from (i) the purely monophasic fluorescence trace, (ii) the absence of intermediate oligomers in the gel permeation profiles, and (iii) the rotational symmetry of the octamer, which gives no indication for the dimer–dimer contact breakages to occur in a preferential order. In fact, this behavior is a common feature of homo-oligomeric proteins with cyclic symmetry (Cantor & Schimmel, 1980).

On the other hand, the pathway of octamer formation has to be a sequence of at least two bimolecular association steps (Jaenicke & Rudolph, 1986), since ternary or even quaternary subunit encounters are unlikely to occur in a dilute solution. Thus, there are two possible mechanisms for the octamerization process: the sequential association of dimers to the complex, involving tetramers and hexamers as intermediates, or octamer formation out of two tetramers.

The fitting of octamerization curves to eq 8 confirms that the assumed model, involving a bimolecular initial association step, is consistent with the data obtained. The bimolecular association rate constant of 318 M^{-1} s^{-1} appears to be about 2 orders of magnitude lower than the k_1 values determined for most other protein–protein associations (Pontius, 1993). For instance, the formation of Y-GAPDH tetramers exhibits a bimolecular association rate constant of 7×10^4 M^{-1} s^{-1}. The slow association of Mi-CK can be explained by considering the collision theory of protein molecules: If an association reaction is diffusion controlled (i.e., any encounter of the reaction partners leads to specific association), k_1 should be around 10^9 M^{-1} s^{-1}. Since generally only a certain fraction of the total protein surface is able to form the specific contact, the rate should be reduced to about 10^3 M^{-1} s^{-1}. The actual value for most proteins is higher than this, because electrostatic forces and nonspecific associations tend to "steer" the collision complex into the appropriate orientation (Pontius, 1993). In the case of Mi-CK, the interaction surface between the dimers is extraordinarily small, with a large, channel-like cavity extending along the 4-fold symmetry axis of the octamer (Schnyder et al., 1991; preliminary X-ray data, W. Kabsch and T. Schnyder, personal communication); consequently, a low k_1 should be expected. The obvious instability of the tetramer is a further indication for the weak interdimer interactions; only the cooperation of four dimer–dimer contacts, with each dimer being held in the structure from two sides, leads to a stable species, the octamer.

Concerning the number of reaction steps occurring on the way from the dimer to the octamer, no definite conclusion can be drawn from the data obtained; however, the lack of a hexameric species in the gel permeation profiles and the high unlikeliness of a reaction sequence involving two unstable intermediates strongly favor the two-step pathway.

From the relatively slow dissociation kinetics of the Mi-CK octamer even under optimal conditions (25–30 °C, low protein concentration, TSAC substrates), the question arises whether the oligomeric transitions of Mi-CK can play a regulatory role in metabolism. Under *in vivo* conditions in the mitochondrial intermembrane space, where the environment is crowded with macromolecules and the Mi-CK concentration as well as the temperature is high, the octameric form of Mi-CK should be strongly favored. Furthermore, no physiological effectors or substrate combinations have been found until now which are capable of inducing a fast octamer decay comparable to the one observed with the TSAC substrates (Wyss, 1992). Until now, there is no evidence for substantial differences in enzymatic activity between dimers and octamers (P. Kaldis, personal communication). These findings suggest that the octamer is the biologically relevant species *in vivo*, the dimer only serving as a building block on the way to the octameric structure. On the other hand, it cannot be fully excluded that in the intermembrane compartment the environment may be sufficiently hydrophobic to destabilize the Mi-CK octamer, so that there still is the possibility of a regulatory function of the octamer–dimer equilibrium (Wallimann et al., 1992; Wyss et al., 1992), e.g., in the regulation of contact site formation (Brdiczka, 1991).

The data presented in this paper show that two Trp residues play well-defined roles in the structure and function of Mi-CK. The limited total number of only five Trp residues in the Mi-CK primary sequence renders it a promising task to use site-directed mutagenesis in order to identify the "active site" and the "interface" Trp residues. The fluorescence spectroscopic assays described here, together with classical enzyme kinetic analyses, should be the tools of choice to characterize the Trp single mutants to be obtained. In turn, the assignment of indole side chains to their sequence positions should be helpful in the alignment of the Mi-CK sequence with the electron density maps from X-ray crystallography which are expected to evolve in the near future (W. Kabsch and T. Schnyder, personal communication).

Furthermore, the fluorescence-based octamer formation and dissociation assays can serve as a convenient means to study the influence of putative physiological and pharmacological effectors on the Mi-CK dimer–octamer equilibrium and to

measure the kinetic octamer stabilities of further Mi-CK mutants, with the opportunity to obtain more structural and functional information about the protein.

ACKNOWLEDGMENT

We would like to thank Dr. E. Furter-Graves for carefully reviewing and refining the manuscript. Prof. H. M. Eppenberger is gratefully acknowledged for his continuous support, and the group of Prof. K. Wüthrich is acknowledged for kindly providing the spectrofluorimeter. We also wish to thank J. Stohner and H. Gross (Laboratory for Physical Chemistry, ETH) for their help in the mathematical treatment of kinetic problems. We are also indebted to E. Zanolla for expert technical support, to Dr. R. Furter for providing the CK expression system and for stimulating discussions and suggestions, and to Dr. M. Wyss, Dr. T. Schnyder, Dr. W. Hemmer, Dr. M. Rojo, and P. Kaldis for contributing their experience, for providing unpublished information, and for many valuable discussions.

REFERENCES

Bartholmes, P., & Jaenicke, R. (1975) *Biochem. Biophys. Res. Commun. 64*, 485–492.

Bartholmes, P., & Jaenicke, R. (1978) *Eur. J. Biochem. 87*, 563–567.

Belousova, L. V., Fedosov, S. N., Rostovtsev, A. P., Zaitseva, N. N., & Myatlev, V. D. (1986) *Biochemistry (Engl. Transl.) 51*, 405–420.

Biermans, W., Bakker, A., & Jacob, W. (1990) *Biochim. Biophys. Acta 1018*, 225–228.

Bradford, M. M. (1976) *Anal. Biochem. 72*, 248–254.

Brdiczka, D. (1991) *Biochim. Biophys. Acta 1071*, 291–312.

Burstein, E. A., Vedenkina, N. S., & Ivkova, M. N. (1973) *Photochem. Photobiol. 18*, 263–279.

Cantor, C. R., & Schimmel, P. R. (1980) *Biophysical Chemistry, Part I*, pp 127–135, W. H. Freeman and Co., New York.

Chien, J.-Y. (1948) *J. Am. Chem. Soc. 70*, 2256–2261.

Eftink, M. R., & Ghiron, C. A. (1976) *Biochemistry 15*, 672–680.

Eftink, M. R., & Ghiron, C. A. (1981) *Anal. Biochem. 114*, 199–227.

Eppenberger, H. M., Perriard, J. C., & Wallimann, T. (1983) *Curr. Top. Biol. Med. Res. 7*, 19–38.

Fedosov, S. N., & Belousova, L. V. (1989) *Biochemistry (Engl. Transl.) 54*, 39–50.

Furter, R., Kaldis, P., Furter-Graves, E. M., Schnyder, T., Eppenberger, H. M., & Wallimann, T. (1992) *Biochem. J. 288*, 771–775.

Jacobs, H., Heldt, H. W., & Klingenberg, M. (1964) *Biochem. Biophys. Res. Commun. 16*, 516–521.

Jacobus, W. E., & Lehninger, A. L. (1973) *J. Biol. Chem. 248*, 4803–4810.

Jaenicke, J., & Rudolph, R. (1986) *Methods Enzymol. 131*, 218–250.

Janin, J., & Chothia, C. (1990) *J. Biol. Chem. 265*, 16027–16030.

Kottke, M., Adams, V., Wallimann, T., Nalam, V. K., & Brdiczka, D. (1991) *Biochim. Biophys. Acta 1061*, 2215–2225.

Marcillat, O., Goldschmidt, D., Eichenberger, D., & Vial, C. (1987) *Biochim. Biophys. Acta 890*, 233–241.

Messmer, C. H., & Kägi, J. H. R. (1985) *Biochemistry 24*, 7172–7178.

Milner-White, E. J., & Watts, D. C. (1971) *Biochem. J. 122*, 727–740.

Parker, C. A., & Barnes, W. J. (1957) *Analyst 82*, 606–618.

Pontius, B. W. (1993) *Trends Biochem. Sci. 18*, 181–186.

Quemeneur, E., Eichenberger, D., Goldschmidt, D., Vial, C., Beauregard, G., & Potier, M. (1988) *Biochem. Biophys. Res. Commun. 153*, 1310–1314.

Rojo, M., Hovius, R., Demel, R., Nicolay, K., & Wallimann, T. (1991a) *J. Biol. Chem. 266*, 20290–20295.

Rojo, M., Hovius, R., Demel, R., Wallimann, T., Eppenberger, H. M., & Nicolay, K. (1991b) *FEBS Lett. 281*, 123–129.

Saks, V. A., Kuznetsov, A. V., Kupriyanov, V. V., Miceli, M. V., & Jacobus, W. E. (1985) *J. Biol. Chem. 260*, 7757–7764.

Schlegel, J. (1989) Ph.D. Thesis, No. 8766, Swiss Federal Institute of Technology, Zurich.

Schlegel, J., Wyss, M., Schürch, U., Schnyder, T., Quest, A., Wegmann, G., Eppenberger, H. M., & Wallimann, T. (1988a) *J. Biol. Chem. 263*, 16963–16969.

Schlegel, J., Zurbriggen, B., Wegmann, G., Wyss, M., Eppenberger, H. M., & Wallimann, T. (1988b) *J. Biol. Chem. 263*, 16942–16953.

Schnyder, T., Engel, A., Lustig, A., & Wallimann, T. (1988) *J. Biol. Chem. 263*, 16954–16962.

Schnyder, T., Gross, H., Winkler, H., Eppenberger, H. M., & Wallimann, T. (1991) *J. Cell Biol. 112*, 95–101.

Stance, G. M., & Deal, W. C., Jr. (1969) *Biochemistry 8*, 4005–4011.

Vasak, M., Nagayama, K., Wüthrich, K., Mertens, M., & Kägi, J. H. R. (1979) *Biochemistry 18*, 5050–5055.

Wallimann, T., Schlösser, T., & Eppenberger, H. M. (1984) *J. Biol. Chem. 259*, 5238–5246.

Wallimann, T., Wyss, M., Brdiczka, D., Nicolay, K., & Eppenberger, H. M. (1992) *Biochem. J. 281*, 21–40.

Wegmann, G., Huber, R., Zanolla, E., Eppenberger, H. M., & Wallimann, T. (1991) *Differentiation 46*, 77–87.

Wyss, M. (1992) Ph.D. Thesis, No. 9777, Swiss Federal Institute of Technology, Zurich.

Wyss, M., & Wallimann, T. (1992) *J. Theor. Biol. 158*, 129–132.

Wyss, M., Smeitink, J., Wevers, R. A., & Wallimann, T. (1992) *Biochim. Biophys. Acta 1102*, 119–166.